Vol. 81 (1992) *ACTA PHYSICA POLONICA A* No 3

SOME STRUCTURE-SENSITIVE PROPERTIES OF NaCl:Ni^{2+} CRYSTALS

D. Nowak-Woźny and M. Suszyńska

W. Trzebiatowski Institute of Low Temperature and Structure Research
Polish Academy of Sciences
Pl. Katedralny 1, 50–950 Wrocław, Poland

(Received December 30, 1991)

The effect of thermal treatment upon the yield strength and some optical absorption parameters were investigated for NaCl crystals containing different amount of divalent nickel. It has been shown that the main changes of the structure-sensitive characteristics occur in two temperature ranges. In the low-temperature range (room temperature–473 K) the yield strength of crystals does change drastically whereas the optical parameters of annealed samples become similar to those characteristic of as-received crystals. On the other hand, the high-temperature annealings (473–673 K) mainly affect the optical characteristics remaining the mechanical ones — more or less similar to those typical of the solution treated state. Some correlations of these effects with the morphology of possible nickel clusters have been shortly discussed.

PACS numbers: 77.40.+i

1. Introduction

It is well-known that divalent impurities (Me^{2+}) enter substitutionally the monovalent lattice of alkali halide crystals (AH) introducing one cation vacancy per each impurity ion. Both entities form the so-called impurity–vacancy (IV) dipoles which — with increasing dopant concentration — form larger objects through aggregation and/or precipitation. The clustering process as well as the dissolution of yet precipitated phases may be followed, for instance, by studying the effects of thermal pretreatment upon some structure-sensitive properties of the AH:Me^{2+} crystal system.

In the present work the mechanical and optical characteristics of NaCl:Ni^{2+} crystals are investigated. The system itself is especially interesting because very few experimental data exist for systems in which the dopant cation is distinctly smaller than the host cation substituted. In such cases there is, in principle, a possibility

that the dopant takes in the lattice either an interstitial- or off-centre-position [1–3], influencing the structure-sensitive properties in a different way than the substitutional impurities are doing.

The optical absorption spectra of NaCl:Ni^{2+} crystals were yet the subject of investigations [4–7]. There are, however, some pecularities in the behaviour found during annealings at 343 K and 573 K [7] which need further more systematic studies. On the other hand, the mechanical characteristics of this crystal system have not yet been studied. It seemed interesting to correlate both types of properties and to look for some correlations with the dispersion form of the dopant changing during the thermal pretreatment of as-received (AR) and solution treated (ST) samples.

2. Experimental details

Nickel-doped NaCl crystals have been grown in our laboratory using the modified Bridgman method diminishing the contamination of any oxygen-containing anion to a level not detectable by conventional optical methods [8].

The content of nickel c_{2+} was determined by exploiting the calibration curve (presented in Fig. 1) $c_{2+} = A\alpha_{248}$, with α_{248} describing the absorption coefficient of the main absorption band. The calibration factor A equals 1.78 for α_{248}

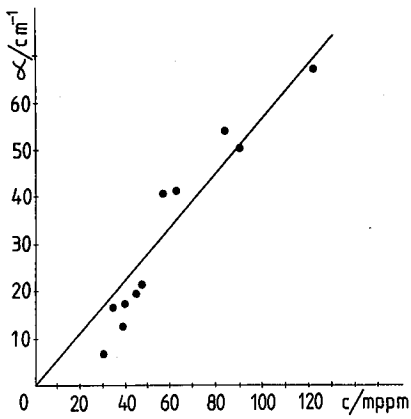

Fig. 1. Relationship between the optical absorption coefficient and nickel concentration estimated by AAS.

expressed in cm^{-1} and c_{2+} — in mole ppm. Atomic absorption analysis (using a Zeiss spectrophotometer) was exploited for a series of standard solutions prepared from high purity metallic nickel dissolved in a mixture of HCl and H_2O_2 containing also such quantity of NaCl which corresponds to an average weight of a NaCl:Ni^{2+} sample tested optically. Optical absorption measurements were performed in the range between 195 and 333 nm using the SPECORD M-40 (Zeiss) spectrophotometer.

Plastic deformation was realized in a uniaxial compression test (along ⟨100⟩) performed in a table 1112-INSTRON machine working at a cross-head speed being equal to 0.05 mm min^{-1}; typical size of samples was $2.5 \times 2.5 \times 8$ mm^3.

All measurements were performed for as-received (AR), solution treated (ST) and additionally annealed (room temperature $\leq T_{an} \leq$ 873 K) ST samples; the solution treatment consisted of 30 minutes of annealing at 873 K (in the air atmosphere) followed by cooling on a cold (at room temperature, RT) copper block. In order to look for some effects of the concentration itself, two different crystals were used; namely, T.6.1 with $c_{2+} \approx 180$ mole ppm and T.6.4 with $c_{2+} \approx 55$ mole ppm.

3. Results and discussion

3.1. Optical data

Results of preliminary studies of the optical absorption of Ni^{2+}- doped NaCl crystals [7] may be summarized as follows:

1. The spectra are dependent on both the dopant concentration and the thermal pretreatment of samples. The differences relate to the number of bands, to the bands' amplitude α [cm^{-1}] and to the position λ [nm] of their maxima.

2. The spectrum of AR samples consists of 2 fairly strong bands (A, C) accompanied by 2 satellites (B, D) of the lower-energy main band (C). In contrast to this picture, all ST samples show exclusively the presence of 2 bands (A, C), only.

3. Storage of ST samples at RT induces a partial recovery of both the intensity and position of the main bands (A, C). However, the low-energy satellite (D) of the C band, present in heavily contaminated AR samples, does not appear in samples stored at RT within an experimentally reasonable time. Only slow cooling of ST samples results in the appearance of this band.

4. After annealings at $T_{an} \leq 473$ K the optical absorption spectra are more or less similar to those typical of AR samples. The main difference between "AR" and "annealed" spectrum relates with the low-energy satellite (D) of band C which does not appear in the spectrum of annealed samples.

5. Annealings at $T_{an} \geq 473$ K induce the transformation of band C into a double one with the maxima positioned at 251 and 276 nm.

We have obtained additional information about the NaCl:Ni^{2+} system for the two crystals isochronally annealed in a wide temperature range. Figure 2a, b presents some of the spectra obtained. It should be noted that practically in the case considered no quantitative differences in the behaviour of the optical spectrum may be quoted. Figure 2c shows three ways of calculation of the integral absorption coefficient α. The values obtained for each of the crystal studied were nearly independent of the thermal history of the sample, suggesting that the number of absorbing centres remains constant during the thermal treatments performed. Moreover, the choice of the background does not influence these values.

It should be emphasized that similar to the previous data [7], the following facts remain not completely clear:

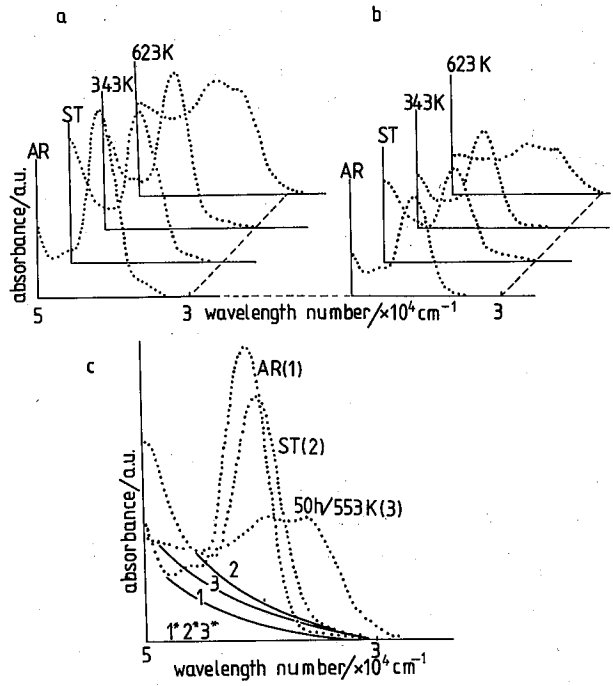

Fig. 2. Optical absorption spectra for the T.6.1 (a, c) and T.6.4 (b) samples.

— whether the shift of λ from 246 through 248 to 251 nm, as observed for the transition from AR through ST to the ST samples annealed at $T_{an} \geq 473$ K, corresponds to the same absorption centres;

— whether the low-energy satellite of band C, present in heavily-doped AR samples (at about 276 nm) corresponds to the band appearing after annealing the ST samples at $T_{an} \geq 473$ K (at about 276 nm).

Figure 3a–c presents the following isochronal plots for the T.6.1 samples: $\lambda(C)$ in nm, α_{248} in cm^{-1} and $\Delta\alpha_n$ in cm^{-1}, respectively, where $\Delta\alpha_n$ denotes the difference between absorption coefficients characteristic for annealed and solution treated samples; $n = 276$ nm (curve 1) and 248 nm (curve 2). The annealing time (t_{an}) for all plots was equal to 50 h; this period has been chosen because for longer t_{an} the spectra did not change in a visible way for the temperatures studied. As can be seen, there are some regularities in the behaviour of the optical characteristics, namely:

— for $T_{an} \in$ (room temperature, 473 K): $\lambda(C)$, α_{248} and $\Delta\alpha_1$ remain constant,

— for $T_{an} \in$ (473 K, 593 K): $\lambda(C)$ and α_{248} decrease whereas $\Delta\alpha_1$ increases,

— for $T_{an} \in$ (593 K, 673 K): $\lambda(C)$ and α_{248} increase whereas $\Delta\alpha_1$ decreases reaching the values characteristic of ST samples.

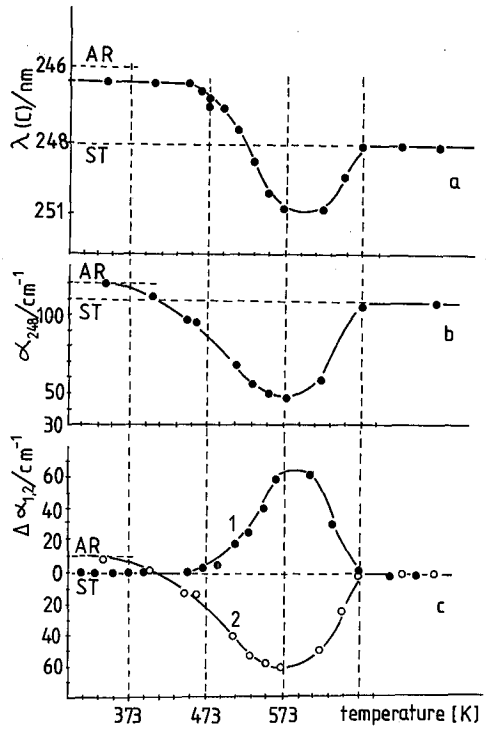

Fig. 3. Isochronal plots of $\lambda(C)$, α_{248} and $\Delta\alpha_n$ where n corresponds to the absorption bands at 248 and 269 nm; $\Delta\alpha_n$ denotes the difference between the α-values for annealed and ST samples.

TABLE I

Some numerical data concerning the optical data.

Sample	Treatment	$\lambda(C)$ [nm]	$\alpha(C)$ [cm^{-1}]	$\lambda(D)$ [nm]	$\Delta\alpha(D)$ [cm^{-1}]
T.6.1	AR	246	120	276	small
	ST	248	110	—	—
	50 h/343 K	247	110	—	—
	50 h/573 K	251	45	269–276	65
T.6.4	AR	246	35	—	—
	ST	248	32	—	—
	50 h/343 K	247	32	—	—
	50 h/573 K	251	18	269–276	14

Table I collects some numerical data. It is interesting to note that the sum of curves 1 and 2 in Fig. 3c is constant and independent of the annealing temperature; i.e. $[\alpha_2(T_{an}) - \alpha_2(ST)] + [\alpha_1(T_{an}) - \alpha_1(ST)] \approx 0$.

3.2. Mechanical characteristics

Figures 4a, b present the isochronal plots of $\Delta\sigma_0(T_{an})$ for both crystals studied; $\Delta\sigma_0$ denotes the difference between yield stress values characteristic of the annealed and solution treated states, i.e. $[\sigma_0(T_{an}) - \sigma_0(ST)]$. The data obtained for 2,5 h $\leq t_{an} \leq$ 80 h are shown.

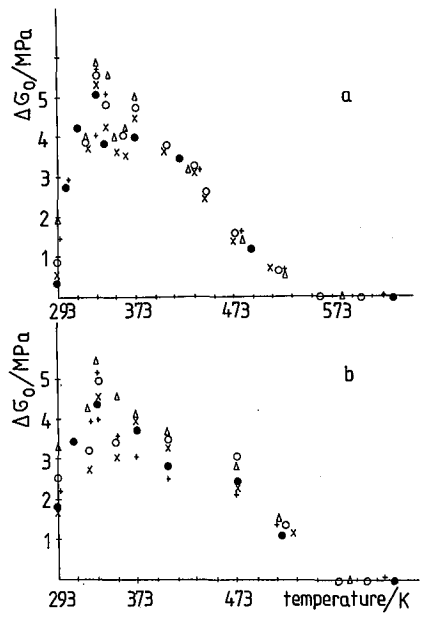

Fig. 4. Isochronal plots of $\Delta\sigma_0 = \sigma_0(T_{an}) - \sigma_0(ST)$ for samples T.6.1 (a) and T.6.4 (b).

Three different temperature ranges can be distinguished for the yield strength changes detected. Namely:

— for $T_{an} \in$ (room temperature, 343 K) $\Delta\sigma_0$ does increase up to about 60 kG cm^{-2} for both samples,

— for $T_{an} \in$ (343 K, 573 K) $\Delta\sigma_0$ decreases up to zero,

— for $T_{an} \geq$ 573 K $\Delta\sigma_0$ remains equal to zero, i.e. σ_0 of annealed samples attains the value characteristic of solution treated ones.

As can be seen, the qualitative character of all isochronal plots presented in Fig. 4 is the same, whereas $\Delta\sigma_0$ increases with t_{an} for each annealing temperature attaining its maximum value at $T_{an} \approx$ 343 K after about 80 h. It is also important to emphasize that the increments of the crystal strength are the same for both concentrations of the dopant. On the basis of the present series of data it is not possible to suggest any reasonable explanation of this behaviour.

3.3. Considerations of the structural correlations

Table II collects some optical and mechanical parameters obtained in the present work as well as some kinetic data given by Andreev et al. [9] for the density of NaCl:Ni^{2+} crystals. As can be seen, major density changes occur only at temperatures above 473 K which roughly separates the temperature ranges where either the mechanical (low temperatures) or optical characteristics (high temperatures) are changing. It has been shown previously [7] that in the high-temperature

TABLE II

Changes of the optical and mechanical characteristics; comparison with the changes of density ($\Delta\rho/\rho_0$ given by Andreev et al. [9]).

T_{an} [K]	$\lambda(C)$ [nm]	α_{248} [cm^{-1}]	$\Delta\alpha_2$ [cm^{-1}]	$\Delta\alpha_1$ [cm^{-1}]	$\Delta\sigma_0$ [MPa]	$\Delta\rho/\rho_0$
room temperature–343	242	120	10	0	↗	const.
343	242	120	10	0	max	const.
343–473	242	120	10	0	↘	const.
473–593	↘	↘	↘	↗	0	↘
593	253	45	−65	65	0	min
593–673	↗	↗	↗	↘	0	↗
> 673	248	110	0	0	0	const. for $T \geq 773$ K

The marks ↘ and ↗ mean the increase and decrease of the parameters considered.

range the main optical absorption band (C) transforms into a double band the second component of which grows at the expenses of the first one. This transformation process suggests that the particles (aggregates and/or precipitates) growing under these experimental conditions (high-temperature annealing followed by rapid cooling to RT) should be rich in vacancies. Large mobility as well as low solubility of the small Ni^{2+} ions in NaCl crystals, cp. [10, 11], are in favour of the precipitation itself, whereas the quenching procedure impedes the flight of vacancies from the precipitated phase volume. Hence, the corresponding decrease of density could be understood in terms of the growth of $NiCl_2$ particles with some vacancy voids included, as was proposed by Andreev et al. [9].

It should be noted that only slow cooling employed after high-temperature annealing results in the formation of "pure" $NiCl_2$ particles, resembling the crystal-growth conditions. On the other hand, it was suggested previously [7] that neither the Suzuki-like phase (proposed by Benedek et al. [12]) nor the mixed $NaNiCl_3$ salt (suggested by Foldvari et al. [6]) are formed in the crystals grown and studied in our laboratory.

Although nothing is known about the morphology of the two types of the $NiCl_2$ particles, it seems reasonable to assume that the vacancy voids are positioned

between the normal layers of the $NiCl_2$ structure which is of $CdCl_2$-type with the unit cell containing only one molecule. The smallest distance between Ni^{2+} ions

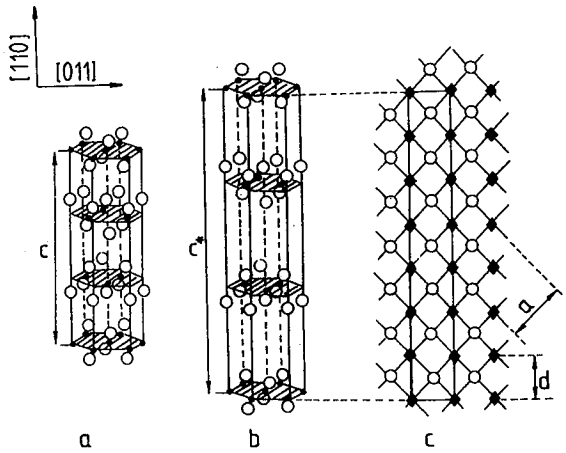

Fig. 5. Figures 5a, b, c present the structures of $NiCl_2$ without vacancies, $NiCl_2$ with some vacancies between the layers and the NaCl matrix, respectively. The dark dots and squares mean the Ni^{2+} and Na^+ cations, whereas the open circles — the Cl^- anions.

is equal to 3.55 Å whereas that between the Cl^- ions — 5.79 Å. This hexagonal network has $z = 3$, $a = 3.55$ Å and $c = 17.35$ Å, cp. Fig. 5. The density of this phase is equal to 3.54 g cm^{-3}, being 1.63 times larger than the density of the matrix. On assuming that the observed density decrease occurs due to the increase of the c-distance between the $CdCl_2$-type layers in the $NiCl_2$ phase, the new c^*-parameter should be 1.58 times larger than the normal c-one.

It should be emphasized that the vacancy-rich $NiCl_2$ phase appears only in the quenched samples, and the growth kinetics of particles (that might be considered as its precursors) obeys a time law characteristic of Ostwald ripening near dislocation lines [7]. In agreement with the observations by Hartmanova et al. [13] the corresponding particles should be preferentially in the form of ⟨110⟩ rods, for which the distortion parameter could be even equal to zero; for instance, $c^* = 1.61\,c$ equals seven times as $d_{\langle 100\rangle}$ — the distance ($d \equiv a\sqrt{2}/2$) in the NaCl lattice.

Finally, one has to note that the "dilution" of the lattice by the vacancy voids included has no remarkable effect upon the mechanical response of samples containing this extraordinary $NiCl_2$ phase in comparison with the effect of dipoles and/or small aggregates.

4. Summary

1. There is no qualitative difference between the optical absorption spectra of the annealed samples with the dopant concentration between 55 and 180 mole ppm, and for annealing temperatures between room temperature and 873 K.

2. Three quantities ($\lambda(C)$, α_{248} and α_{273}) do change in a similar way during isochronal annealings at all annealing temperatures with an extremum at 593 K and constant values for $T_{an} \in (RT, 473\ K)$ and $T_{an} \geq 673$ K.

3. The isochronal plots of $\Delta\sigma_0(T_{an})$ have their maximum values at about 343 K, and above 573 K $\Delta\sigma_0$ equals zero, i.e. the behaviour of $\Delta\sigma_0$ is opposite to the behaviour of the optical characteristics.

4. Comparing the kinetic data with changes of the crystal density, one has postulated that thermal pretreatment of ST samples may result in the formation of $NiCl_2$ phases with and without some vacancies included. The vacancy-rich particles are probably in the form of ⟨110⟩ rods.

Acknowledgments

The authors wish to express their thanks to Mrs. T. Morawska-Kowal for growth of the crystals.

References

[1] W. Dreyfus, *Phys. Rev.* **121**, 1675 (1961).

[2] W. Dreyfus, R.B. Laibowitz, *Phys. Rev.* **148**, 816 (1966).

[3] C. Bucci, *Phys. Rev.* **164**, 1200 (1967).

[4] K. Polak, *Z. Phys.* **223**, 338 (1969).

[5] T. Nasu, Y. Asano, *J. Phys. Soc. Jpn.* **27**, 264 (1969).

[6] I. Foldvari, R. Voszka, Z. Morlin, *Phys. Status Solidi B* **69**, 235 (1978).

[7] D. Nowak-Woźny, M. Suszyńska, M. Szmida, R. Capelletti, to be published.

[8] R. Voszka, J. Tarjan, L. Berkes, J. Krajsovszky, *Kristall u. Technik* **1**, 426 (1966).

[9] G.A. Andreev, M. Hartmanova, V.A. Klimov, *Phys. Status Solidi A* **41**, 697 (1977).

[10] P. Suptitz, J. Teltow, *Phys. Status Solidi* **23**, 9 (1967).

[11] M. Kaderka, *Czech. J. Phys. B* **18**, 1222 (1968); ibid. **19**, 530 (1969).

[12] G. Benedek, J.M. Calleja, R. Capelletti, A. Breitschwerdt, *J. Phys. Chem. Solids* **45**, 741 (1984).

[13] M. Hartmanova, G.A. Andreev, V.A. Klimov, *Phys. Stat. Solidi A* **41**, 679 (1977).